A SAXS–WAXD Study on the Mesomorphic-α Transition of Isotactic Polypropylene

Carla Marega, Valerio Causin, Antonio Marigo

Dipartimento di Scienze Chimiche, Università di Padova, via Marzolo 1, 35131 Padova, Italy

Received 26 July 2007; accepted 2 January 2008
DOI 10.1002/app.28017
Published online 19 March 2008 in Wiley InterScience (www.interscience.wiley.com).

ABSTRACT: The smectic-α transition of iPP was studied by wide angle X-ray diffraction (WAXD) and small angle X-ray scattering (SAXS). WAXD and SAXS patterns were taken at different temperatures during the transition. Two different approaches were taken in the analysis of SAXS data: the correlation function and a fitting method based on theoretical distribution models. Up to 80°C just smectic phase was observed, whereas beyond that temperature α lamellae appeared and the two populations of lamellae were found to coexist in the sample. The new α phase population stemmed from within the preexistent smectic stacks, according to a lamellar insertion model. α lamellae thickened to a larger extent than the smectic phase, that just underwent thermal expansion. Results were consistent with a mechanism of transformation involving a rearrangement of the chains without a melting-recrystallization process. © 2008 Wiley Periodicals, Inc. J Appl Polym Sci 109: 32–37, 2008

Key words: poly(propylene); smectic phase; crystallization; SAXS; WAXS; X-ray

INTRODUCTION

When crystallized from the melt, isotactic polypropylene (iPP) chains adopt a 3_1 helical conformation and can organize themselves into several spatial arrangements giving rise to three different polymorphs: α, β, and γ phases.[1–4] The crystalline structures of these phases differ by the combinations of left- and right-handed helices and up and down stems concerning the CH_3 group.[5] The α polymorph is the most commonly occurring, whereas the appearance of β and γ forms is favored by special crystallization conditions and adequate nucleants. Along with these well-known and studied crystalline phases, there is also a ''mesomorphic'' phase, which can be obtained by rapid quenching of iPP. Although it has been quite widely investigated, its nature remains somewhat obscure. Natta described the structure as ''smectic,'' i.e., composed of parallel 3_1 helices with a disordered packing along the perpendicular to the chain axes.[1] Other explanations focused on defects of the crystal: it was described as ''paracrystalline,''[6,7] conformational disorder crystal[8] or as consisting of very small crystallites.[9–13] The mesomorphic phase has an intermediate degree of ordering between the amorphous and crystalline phase and is composed of a collection of helical chain segments with random helical hands.[1,14] At a nanometric scale, two morphologies were postulated. On the basis of transmission electron microscopy (TEM), a globular structure, with polygonal or spherical nodules was described,[5,12,15–17] whereas SAXS experiments were more coherent with a lamellar morphology.[18–21]

Another interesting feature of the mesomorphic phase of iPP is that it undergoes a phase transition to the monoclinic α phase.[11,14–24] This transition was explained according to different models. Hsu et al.[15] reported, during the transition, an increase in the size of mesomorphic nodules that brings about a coalescence into a fibrillar morphology. This would happen as soon as polymer chains are mobile enough, due to thermal motion, to rotate and improve their packing. Ferrero et al.[11] and Jin et al.[23] confirmed this explanation, postulating a mechanism in which the mesophase undergoes melting and a subsequent recrystallization into regular α phase. Wang et al.[14] argued that the transition from mesomorphic to α is essentially a correction of the wrongly handed adjacent helices of the mesomorphic phase into the correctly registered ones of the α unit cell. The change of the helical structure from one hand to the other is associated to a very significant reconfiguration of the chain, viz. a melting process. So Wang et al. proposed that the transition follows a sequence that begins with a partial melting process, that leaves intact the local lateral ordering of the chains while allowing a correct registration of their helical hands, and is followed by a secondary nucleation that transforms mesomorphic nodules into lamellae.[14] If the structure of the mesomorphic phase is described as paracrystalline, with a monoclinic-like local ordering, the transition to the monoclinic α form can happen with relatively little

Correspondence to: C. Marega (carla.marega@unipd.it).

rearrangement, as suggested by O'Kane et al.[18] This can lead to Martorana's model,[20,21] consistent with Marigo et al.'s results,[19] according to which annealing of the mesomorphic phase can bring about the thickening of already existing α phase lamellae at the expenses of amorphous regions and the extension of order of the mesomorphic phase to larger ranges typical of the α phase.[20,21] These new lamellae can either form as an aggregation of mesomorphic domains or by a conventional secondary crystallization.[17]

Among the most controversial issues of the mechanism of the smectic-α transition, there is therefore the existence of a melting-recrystallization phenomenon. Also of interest for shedding light on the mechanistic details of the transformation is the description of the morphology of the lamellae of the α and of the smectic phase.

The purpose of this work is to elucidate these structural and morphological aspects of the mesomorphic-α transition, by the use of wide angle X-ray diffraction (WAXD) and SAXS. An understanding of these issues can in fact be of help in the control of the semicrystalline structure of iPP and therefore of its structure. Moreover, this topic deserves attention particularly because recent results showed that homogeneously nucleated iPP in confined nanoparticles crystallizes in the smectic form.[23] This pointed to this mesomorphic phase as a precursor of the nuclei of crystallization. It has been advocated by some authors that the nucleation and growth phases of the polymer crystallization mechanism can involve an intermediate smectic phase,[25–27] so it is of the utmost importance to have as many structural and morphological details regarding the subsequent transition from the smectic to the final crystalline phase.

EXPERIMENTAL

Samples and sample preparation

iPP was produced by Basell Polyolefins ($\bar{M}_w = 350,000$, $\bar{M}_n = 46,900$). The cast film was prepared in a single-screw Plasticizer MKII extruder, working at 48–49 rpm, at a melt temperature of 260°C, and with a slow roll at 20–30°C (rotation speed 0.2 m/min).[19]

WAXD

WAXD patterns were recorded by a Rigaku Geigerflex D/MAX-C powder diffractometer (CuKα radiation) equipped with a controlled temperature sample holder. Measurements were taken at room temperature, 60, 80, 100, 120, 140, 150, and 160°C, the heating rate was 20°C/min. The angular range for the measurements was 11–26° 2θ. A least-square fit procedure was applied according to Hindeleh and Johnson[28] to reproduce WAXD profiles and to determine the degree of crystallinity.

SAXS

The SAXS patterns of the samples were recorded by an MBraun system, utilizing a CuK_α radiation from a Philips PW 1830 X-ray generator. The data were collected by a position sensitive detector, in the scattering angular range 0.1–5.0° 2θ.

The sample was equipped with a controlled temperature sample holder and measurements were taken at the same temperatures as in WAXD experiments. Each SAXS acquisition lasted 450 s. Data were corrected for blank scattering and successively the one-dimensional scattering function was obtained by the Lorentz correction $I_1(s) = 4\pi s^2 I(s)$, where $I_1(s)$ is the one-dimensional scattering function and $I(s)$ the experimental intensity function, being $s = (2/\lambda)\sin\theta$.

SAXS data analysis

Two approaches were adopted in the interpretation of SAXS data. The first was based on the correlation function.[29] The first maximum of the correlation function yields the long period D_γ, whereas by the construction of the autocorrelation triangle, the numerical averages of the thicknesses of the amorphous and crystalline layers can be obtained, provided that the volume crystallinity is known from some other complementary technique such as WAXD. The thickness of the transition layer was evaluated according to Ruland.[30]

The second approach for the evaluation of the SAXS patterns was carried out according to some theoretical distribution models[31,32] and referring to the Hosemann model,[33] that assumes the presence of lamellar stacks having an infinite side dimension. This assumption takes into account a one-dimensional electron density change along the normal direction to the lamellae.

The intensity profile was evaluated as:

$$I(s) = I^{\mathrm{I}}(s) + I^{\mathrm{II}}(s)$$

where:

$$I^{\mathrm{I}}(s) = \frac{(\rho_C - \rho_A)^2}{4\pi^2 s^2 D} \times \frac{|1 - F_C|^2(1 - |F_A|^2) + |1 - F_A|^2(1 - |F_C|^2)}{(1 - F_C F_A)^2}$$

$$= \frac{(\rho_C - \rho_A)^2}{2\pi^2 s^2 DN} \times Re\left\{\frac{F_A(1 - F_C)^2(1 - (F_C F_A)^N)}{(1 - F_C F_A)^2}\right\} \times I^{\mathrm{II}}(s)$$

In these equations, F_C and F_A represent the Fourier transforms of the distribution functions of the crystal-

line (*C*) and of the amorphous (*A*) regions, ρ_C and ρ_A are the electron densities of the crystalline and amorphous regions, respectively, *N* is the number of layers in the system and *D* the average long period. A fitting procedure of the calculated one-dimensional scattering functions with the experimental ones allows to optimize the values of the high and low density region thicknesses. Crystallinity (ϕ_{SAXS}) was evaluated as the ratio between the thickness of the high density regions over the long period $D = C + A$.

RESULTS AND DISCUSSION

WAXD patterns were acquired at seven different temperatures, chosen to cover as uniformly as possible the interval between room temperature and the melting point. The results are reported elsewhere.[19] In particular, below 80°C only the typical profile of the iPP smectic phase was visible, with two broad bands at about 14.8 and 21.2° 2θ.[1,15,18] Beyond 80°C the characteristic peaks of the α phase begin to appear, meaning that the smectic-α transition has begun.

SAXS was also performed on the samples and Figure 1 shows the obtained patterns. As already said in the experimental section, two approaches were adopted in the interpretation of SAXS data. The first was based on the correlation function,[29] the second was that of fitting experimental patterns by functions based on theoretical distribution models.[31–33] This method was somewhat preferable because its results are solely based on SAXS. In the correlation function data treatment, in fact, WAXD crystallinity is employed for the estimation of the lamellar thickness, while the fitting technique yielded lamellar parameters only on the basis of the SAXS profile. Moreover, the fitting method allows to obtain a larger number of morphological parameters, like the distribution of the thicknesses and of the crystallinity associated to the lamellar stacks, that can not be evaluated by the analysis of the correlation function.

TABLE I
Morphological Features of the Lamellar Stacks Determined by the Correlation Function at Different Temperatures

Temperature (°C)	D_γ (Å)	C_γ (Å)	A_γ (Å)	E (Å)
25	87	24	63	11
60	86	25	61	10
80	87	30	57	10
100	90	33	57	10
120	93	40	53	8
140	114	53	61	8
160	196	89	107	12

D_γ is the long period, C_γ and A_γ are the thicknesses of the crystalline and amorphous layers according to a pseudo-biphasic model, and *E* is the transition layer.

The reliability of the fitting method was also successfully checked by comparison with TEM measurements.[34,35] The results obtained by the correlation function method are shown in Table I and Figure 2. It has already been observed on analogous samples[19] that the long period increases with increasing temperature. Up to about 100°C, the marginal increase in D_γ should be attributed to thermal expansion. The sharp rise of D_γ beyond 100°C can be explained by the fact that the smaller and less stable lamellae begin to melt, skewing the average D_γ toward larger values.[19] Another datum that can be obtained from Figure 2 is that the first peak of the correlation function broadens as temperature rises. This can be qualitatively associated to a broader distribution of periodicities[29] that can be due, among other factors, to a nonuniform thermal dilatation for crystalline and amorphous zones or the gradual melting, especially beyond 100°C, of the less stable lamellae. The trend of the thicknesses of the amorphous and crystalline layers obtained by the analysis of the correlation function confirms what was observed above. The amorphous layer thickness decreases slightly, whereas the crystalline thickness increases specularly,

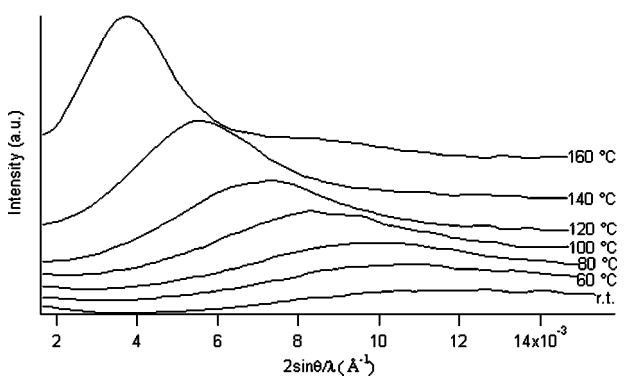

Figure 1 SAXS profiles of the sample, acquired during the temperature-dependent experiment.

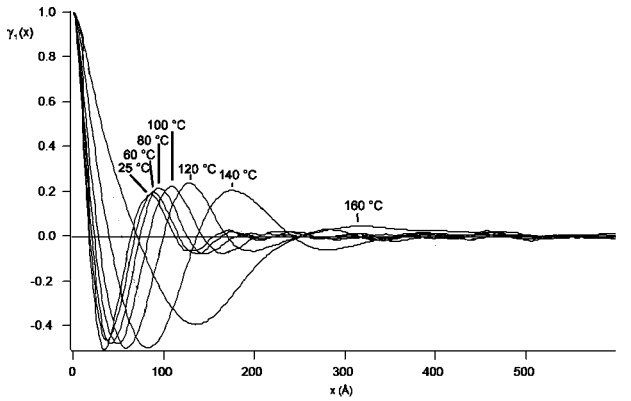

Figure 2 Correlation functions obtained from the SAXS patterns of the sample at the indicated temperatures.

TABLE II
Crystalline (*C*) and Amorphous (*A*) Layers Average Thicknesses, Long Period (*D*), Thickness Distribution Values (σ_C/C, σ_A/*A* and σ_D/D) Determined by SAXS

Temperature (°C)	D_1 (Å)	C_1 (Å)	A_1 (Å)	σ_{D_1}/D_1	σ_{C_1}/C_1	σ_{A_1}/A_1	D_2 (Å)	C_2 (Å)	A_2 (Å)	σ_{D_2}/D_2	σ_{C_2}/C_2	σ_{A_2}/A_2	ϕ_{SAXS} (%)
25	76	20	56	0.39	0.50	0.50	–	–	–	–	–	–	26
60	86	25	61	0.35	0.46	0.46	–	–	–	–	–	–	29
80	91	29	62	0.34	0.45	0.45	–	–	–	–	–	–	32
100	105	40	65	0.34	0.47	0.47	64	24	40	0.31	0.43	0.43	38
120	133	60	73	0.26	0.37	0.37	83	37	46	0.33	0.46	0.46	45
140	164	82	82	0.25	0.35	0.35	98	49	49	0.33	0.46	0.46	50
160	237	124	113	0.27	0.38	0.38	115	60	55	0.35	0.49	0.49	52

Subscripts 1 and 2 denote the first and second lamellar population, respectively.

up to about 120°C, consistently with a hypothesis of crystallization and lamellae formation. Beyond 120°C the onset of melting of the thinnest lamellae determines an increase in amorphous thickness. At the same time, the crystalline layer keeps thickening, because the smectic-α transition becomes more important as temperature rises and because the melting of thinner lamellae increases its average thickness. A contribution from thermal expansion is expected to be quite significant, especially in the increase of the amorphous layer, since the thermal expansion coefficient of the amorphous layer has been reported to be larger than that for the crystalline phase.[36] Table I also shows that the thickness of the transition layer does not undergo very significant changes with temperature.

The second approach of analysis of SAXS data yielded further detail for the understanding of the transition. Results are showed in Table II. A very different morphology is found above and below 80°C. At lower temperatures, just one population of lamellar stacks is observed, whereas from 100°C a second population appears. This behavior is consistent with the reports of Martorana and colleagues.[20,21] These researchers were the first to demonstrate the occurrence of two different long period values, relative to the smectic and α phase. They observed that the smectic population did not change its long period with annealing, whereas α lamellar stacks increased their periodicity, probably at the expenses of the mesomorphic phase.[20,21] In their measurements, these researchers found the occurrence of both phases in the pristine material, even though the WAXD pattern revealed the presence of only smectic phase. Probably the microstructure of their iPP samples and the processing imposed were not optimal to obtain 100% mesomorphic phase. Their work confirmed indeed that SAXS can detect much lower levels of crystallinity than WAXD.[14,17] Our results show that below 80°C just the mesomorphic phase is present. Beyond that temperature, the smectic-α transition begins and the second population, due to α phase lamellae, appeared. Figures 3–5 compare the results obtained by the two methods of interpretation of SAXS data. A good accord with the two techniques is evident up to 80°C. For higher temperatures, the data obtained by the correlation function are in between those of the two populations. Although both methods describe the lamellar morphology of the sample, the fitting technique appears to be more suitable to study its finer details. A

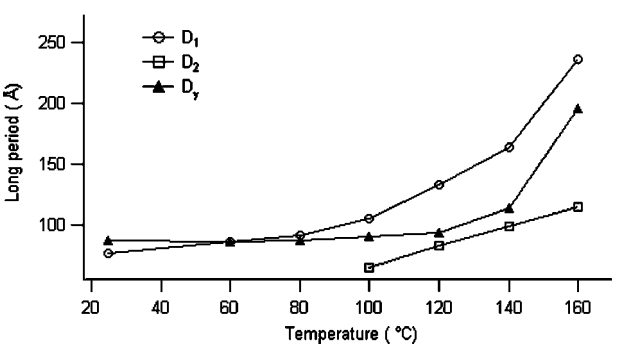

Figure 3 Long period as a function of temperature, measured by the fitting method (D_1 is the long period of the first population, and D_2 is that of the second population) and by the correlation function method (D_γ).

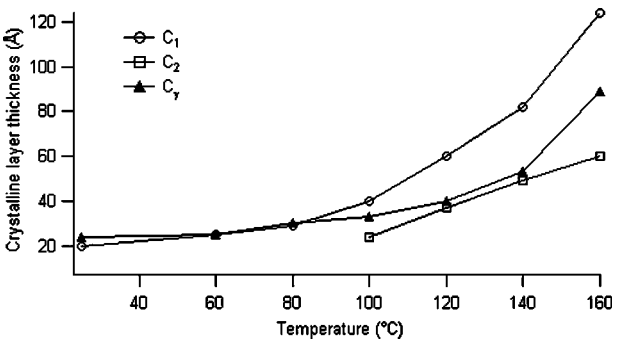

Figure 4 Thickness of the crystalline layer as a function of temperature, measured by the fitting method (C_1 is the thickness of the first population, and C_2 is that of the second population) and by the correlation function method (C_γ).

steeper increase in the lamellar features is seen in population 1, the one relative to the α polymorph, whereas population 2 increases less but more constantly, probably due to thermal expansion. It is very interesting to see that even at the highest temperature, very close to complete isotropization, the smectic population resists. This is consistent with a smectic-α mechanism of transformation that requires a rearrangement of the chains[15,18] without a melting-recrystallization process. If the transition passed in fact through melting of the mesomorphic phase, this would be easily detectable with a sharp increase in the amorphous thickness of the second population, which was not observed by us. About the location of the new lamellar stacks of the α phase, Marega et al.[37] recently proposed a model to infer if new stacks grow according a lamellar insertion or a dual lamellar stack scheme, on the basis of the trend of the difference between WAXD and SAXS crystallinities. Comparing the volumetric crystallinities measured by both these techniques, in fact, differences are usually noted, the one obtained by WAXD being lower than that yielded by SAXS. This divergence can be explained considering the difference between the two techniques. WAXD allows the detection of all the crystalline forms in the sample, whereas SAXS is only sensitive to the regions organized in lamellar stacks. The lower crystallinity obtained by WAXD is thus due to amorphous domains that are external to lamellar stacks, not detected by SAXS. In the lamellar insertion model, the second population of subsidiary lamellae exists within the main lamellar stacks, whereas in the dual stack model, the second population is a separate entity with respect to the main lamellar stacks.[38–41] If a lamellar insertion holds, WAXD crystallinity will increase as a function of the advancement of crystallization, either in terms of time or temperature, by a lesser extent than SAXS

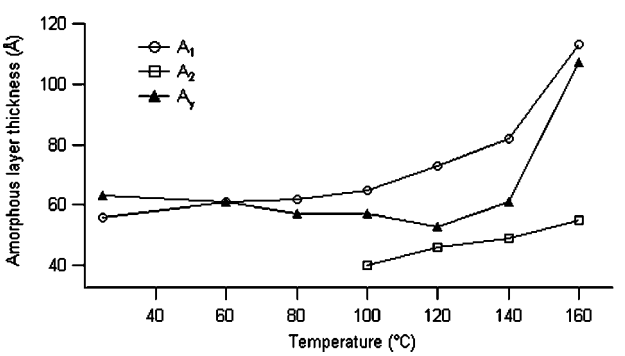

Figure 5 Thickness of the amorphous layer as a function of temperature, measured by the fitting method (A_1 is the thickness of the first population, and A_2 is that of the second population) and by the correlation function method (A_γ).

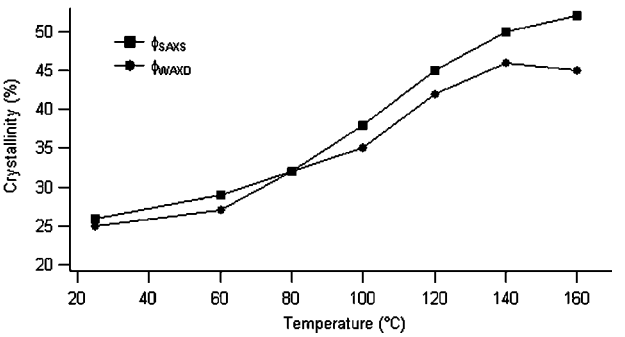

Figure 6 Trend of the degree of crystallinity as measured by SAXS (ϕ_{SAXS}) and WAXD (ϕ_{WAXD}) as a function of temperature.

crystallinity, because of a ''dilution'' effect by extralamellar amorphous.[37] On the other hand, formation of new lamellae outside the existing lamellar stacks determines a decrease in the quantity of extralamellar amorphous material and therefore a more rapid increase in WAXD rather than SAXS crystallinity.[37] Figure 6 shows that the difference between WAXD and SAXS crystallinity widens with temperature, so experimental data are more consistent with an α phase lamellar population stemming from within smectic stacks. This would confirm that the mesomorphic phase can indeed serve as a precursor of polymeric crystals.[25–27] It should be noted that in a previous investigation it was excluded that new lamellae could be produced within existing lamellar stacks.[19] In that case, though, less detailed interpretative models were used, that did not take into account the existence of two populations and conclusions were taken only on the basis of the trend of the SAXS long period.

CONCLUSIONS

The mesomorphic-α transition of iPP was studied by WAXD and SAXS. Two different approaches were taken in the analysis of SAXS data. Below 80°C just one population of lamellae, that of the smectic phase, was observed, whereas beyond that temperature α lamellae appeared and the two populations were found to coexist in the sample. The thickening of α lamellae was much more extensive than that of the smectic phase, that just underwent thermal expansion. Results were consistent with a mechanism of transformation involving a rearrangement of the chains without a melting-recrystallization process. The new α phase lamellar population stemmed from within the preexistent smectic stacks.

The authors gratefully thank Basell Polyolefins Italia for the supply of samples.

References

1. Natta, G.; Corradini, P. Nuovo Cimento (Suppl) 1960, 15, 40.
2. Turner Jones, A.; Aizlewood, J. M.; Beckett, D. R. Makromol Chem 1964, 75, 134.
3. Lotz, B.; Wittmann, J. C.; Lovinger, A. J. Polymer 1996, 37, 4979.
4. Moore, E. P.; Polypropylene Handbook; Hanser: Munich, 1996.
5. Konishi, T.; Nishida, K.; Kanaya, T.; Kaji, K. Macromolecules 2005, 38, 8749.
6. Miller, R. L. Polymer 1960, 1, 135.
7. Hosemann, R. Acta Cryst 1951, 4, 520.
8. Grebowicz, J.; Lau, S.-F.; Wunderlich, B. J Polym Sci Polym Symp 1984, 71, 19.
9. Gailey, J. A., Ralston, R. H. SPE Trans 1964, 4, 29.
10. Caldas, V.; Brown, G. R.; Nohr, R. S.; MacDonald, J. G.; Raboin, L. E. Polymer 1994, 35, 899.
11. Ferrero, A.; Ferracini, E.; Mazzavillani, A.; Malta, V. J.; Macromol Sci Phys 2000, B39, 109.
12. Androsch, R.; Wunderlich, B. Macromolecules 2001, 34, 5950.
13. Song, Y.; Nitta, K.; Nemoto, N. Macromolecules 1955 2003, 36.
14. Wang, Z.-G.; Hsiao, B. S.; Srinivas, S.; Brown, G. M.; Tsou, A. H.; Cheng, S. Z. D.; Stein, R. S. Polymer 2001, 42, 7561.
15. Hsu, C. C.; Geil, P. H., Miyaji, H.; Asai, K. J Polym Sci Polym Phys Ed 1986, 24, 2379.
16. Ran, S.; Zong, X.; Fang, D.; Hsiao, B. S.; Chu, B.; Phillips, R. A. Macromolecules 2001, 34, 2569.
17. Zia, Q.; Androsch, R.; Radusch, H. -J.; Piccarolo, S. Polymer 2006, 47, 8163.
18. O'Kane, W. J; Young, R. J; Ryan, A. J; Bras, W.; Derbyshire, G. E.; Mant, G. R. Polymer 1994, 35, 1352.
19. Marigo, A.; Marega, C.; Zannetti, R.; Fichera, A.; Ferrari, P. Macromol Chem Phys 1995, 196, 3577.
20. Gerardi, F.; Piccarolo, S.; Martorana, A.; Sapoundjieva, D. Macromol Chem Phys 1997, 198, 3979.
21. Martorana, A.; Piccarolo, S.; Sapoundjieva, D. Macromol Chem Phys 1999, 200, 531.
22. Minami, S.; Tsurutani, N.; Miyaji, H.; Fukao, K.; Miyamoto, Y. Polymer 2004 45, 1429.
23. Jin, Y.; Hiltner, A.; Baer, E.; Masirek, K.; Piorkowska, E.; Galeski, A. J Polym Sci Polym Phys Ed 2006, 44, 1796.
24. Cao, J; Sbarski, I. Polymer 2006, 47, 27.
25. Strobl, G. Eur Phys J E 2000, 3, 165.
26. Muthukumar, M. Philos Trans R Soc London Ser A 2003, 361, 539.
27. Li, L.; de Jeu, W. H. Macromolecules 2003, 36, 4862.
28. Hindeleh, A. M.; Johnson, D. J. J Phys D: Appl Phys 1971, 4, 259.
29. Strobl, G. R.; Schneider, M. J Polym Sci Polym Phys Ed 1980, 18, 1343.
30. Ruland, W. J Appl Cryst 1971, 4, 70.
31. Blundell, D. J Polym 1978, 19, 1258.
32. Marega, C.; Marigo, A.; Cingano, G.; Zannetti R.; Paganetto, G. Polymer 1996, 37, 5549.
33. Hosemann R.; Bagchi, S. N. Direct Analysis of Diffraction by Matter; North Holland: Amsterdam, 1962.
34. Marigo, A.; Marega, C.; Zannetti, R.; Sgarzi, P. Eur Polym Mater 1998, 34, 597.
35. Causin, V.; Marega, C.; Marigo, A.; Ferrara, G. Polymer 2005, 46, 9533.
36. Schoutern, P.; Vandermarliere, M.; Riekel, C.; Kock, M. H. J.; Groeninckx, G; Reynaers, H. Macromolecules 1989, 22, 237.
37. Marega, C.; Causin, V.; Marigo, A. Macromol Res 2006, 14, 588.
38. Lattimer, M. P.; Hobbs, J. K.; Hill, M. J.; Barham, P. J. Polymer 1992, 33, 3971.
39. Krüger, K. N.; Zachmann, H. G. Macromolecules 1993, 26, 5202.
40. Hsiao, B. S.; Gardner, K. H.; Wu, D. Q. Polymer 1993, 34, 3996.
41. Verma, R.; Marand, H.; Hsiao, B. Macromolecules 1996, 29, 7767.